SIAM J. Sci. Comput.
Vol. 27, No. 2, pp. 714–739

PARALLEL LAGRANGE–NEWTON–KRYLOV–SCHUR METHODS FOR PDE-CONSTRAINED OPTIMIZATION. PART II: THE LAGRANGE–NEWTON SOLVER AND ITS APPLICATION TO OPTIMAL CONTROL OF STEADY VISCOUS FLOWS*

GEORGE BIROS† AND OMAR GHATTAS‡

Abstract. In part I of this article, we proposed a Lagrange–Newton–Krylov–Schur (LNKS) method for the solution of optimization problems that are constrained by partial differential equations. LNKS uses Krylov iterations to solve the linearized Karush–Kuhn–Tucker system of optimality conditions in the full space of states, adjoints, and decision variables, but invokes a preconditioner inspired by reduced space sequential quadratic programming (SQP) methods. The discussion in part I focused on the (inner, linear) Krylov solver and preconditioner. In part II, we discuss the (outer, nonlinear) Lagrange–Newton solver and address globalization, robustness, and efficiency issues, including line search methods, safeguarding Newton with quasi-Newton steps, parameter continuation, and inexact Newton ideas. We test the full LNKS method on several large-scale three-dimensional configurations of a problem of optimal boundary control of incompressible Navier–Stokes flow with a dissipation objective functional. Results of numerical experiments on up to 256 Cray T3E-900 processors demonstrate very good scalability of the new method. Moreover, LNKS is an order of magnitude faster than quasi-Newton reduced SQP, and we are able to solve previously intractable problems of up to 800,000 state and 5,000 decision variables at about 5 times the cost of a single forward flow solution.

Key words. sequential quadratic programming, adjoint methods, PDE-constrained optimization, optimal control, Lagrange–Newton–Krylov–Schur methods, Navier–Stokes, finite elements, preconditioners, indefinite systems, nonlinear equations, parallel algorithms

AMS subject classifications. 49K20, 65F10, 65K05, 65K10, 65J22, 65N55, 65W10, 65Y05, 65Y20, 76D05, 76D07, 76D55, 90C52, 90C55, 90C90, 93C20

DOI. 10.1137/S1064827502415661

1. Introduction.

In part I of this two-part article [3] we proposed a Newton–Krylov method for solution of the optimality system stemming from the optimization of systems governed by partial differential equations (PDEs). We concentrated our discussion on the inner iteration: the solution of the linear system associated with a Newton step on the Karush–Kuhn–Tucker (KKT) optimality conditions. The algorithm is based on a Krylov solver combined with a family of Schur-type preconditioners that are equivalent to an approximate quasi-Newton reduced SQP (QN-RSQP) step. We termed the method *Lagrange–Newton–Krylov–Schur* (LNKS), a concatenation of *Lagrange–Newton* for the outer iteration and *Krylov–Schur* for the inner iteration. We also provided theoretical and numerical evidence that these preconditioners work very well by considering several linearly-constrained quadratic optimization problems, namely those involving boundary control of Stokes flows with flow-matching

*Received by the editors October 9, 2002; accepted for publication (in revised form) November 17, 2004; published electronically November 15, 2005. This work is a part of the Terascale Algorithms for Optimization of Simulations (TAOS) project at CMU, with support from NASA grant NAG-1-2090, NSF grant ECS-9732301 (under the NSF/Sandia Life Cycle Engineering Program), and the Pennsylvania Infrastructure Technology Alliance. Computing services on the Pittsburgh Supercomputing Center's Cray T3E were provided under PSC grant BCS-960001P.
http://www.siam.org/journals/sisc/27-2/41566.html

†Courant Institute of Mathematical Sciences, Department of Computer Science, New York University, New York, NY 10012 (biros@cs.nyu.edu).

‡Ultrascale Simulation Laboratory, Departments of Biomedical Engineering and Civil & Environmental Engineering, Carnegie Mellon University, Pittsburgh, PA 15213 (oghattas@cs.cmu.edu).

and dissipation-type objectives.

In part II, we present algorithmic components of the LNKS method related to the (outer) Lagrange–Newton solver, including such globalization strategies as line search, quasi-Newton safeguarding, and parameter continuation, and inexactness in the inner linear solver and its interaction with the line search. We assess performance of the LNKS method on several more stringent test problems that contain many features of the most challenging PDE-constrained optimization problems: three-dimensional unstructured meshes, multicomponent coupling, large problem size, nonlinearity, and ill-conditioning. The underlying problem class is optimal control of a viscous incompressible fluid by boundary velocities, which is of both theoretical and industrial interest.

Following part I, we refer to the unknown PDE field quantities as the *state variables*; the PDE constraints as the *state equations*; solution of the PDE constraints as the *forward problem*; the inverse, design, or control variables as the *decision variables*; and the problem of determining the optimal values of the inverse, design, or control variables as the *optimization problem*.

The paper is organized as follows. In section 2 we briefly review the problem formulation. We then discuss algorithmic issues related to Lagrange–Newton methods and in particular globalization methodologies. We give details on three globalization techniques to enhance robustness in the LNKS method: line search, safeguarding LNKS steps with (approximate) QN-RSQP steps, and continuation. We also discuss inexact Newton methods and how they interact with a merit function line search. In section 3 we present the full globalized LNKS algorithm. Section 4 formulates the optimal control problem for the Navier–Stokes equations and presents results for a Poiseuille flow, a flow around a cylinder, and a flow around a Boeing 707 wing.

Note on notation. We use boldface characters to denote vector-valued functions and vector-valued function spaces. We use roman characters to denote discretized quantities and italics for their continuous counterparts. For example, $\boldsymbol{u}$ will be the continuous velocity field and $\mathbf{u}$ will be its discretization. Greek letters are overloaded and whether we refer to the discretization or the continuous fields should be clear from context. We also use $+$ as a subscript or superscript to denote variable updates within an iterative algorithm.

2. Globalization and inexactness of the LNKS method.

In this section we consider strategies for globalizing the Newton iteration at the heart of the LNKS method, as well as opportunities for introducing inexactness in the solution for a Newton step. Let us revisit the constrained optimization problem formulation,

$$\min_{\mathbf{x}\in\mathbb{R}^N} f(\mathbf{x}) \quad \text{subject to } \mathbf{c}(\mathbf{x}) = \mathbf{0}, \tag{2.1}$$

where $\mathbf{x} \in \mathbb{R}^N$ are the optimization variables, $f : \mathbb{R}^N \to \mathbb{R}$ is the objective function, and $\mathbf{c} : \mathbb{R}^N \to \mathbb{R}^n$ are the constraints. In our context these constraints are discretizations of the state equations. The Lagrangian,

$$\mathcal{L}(\mathbf{x}, \boldsymbol{\lambda}) := f(\mathbf{x}) + \boldsymbol{\lambda}^T \mathbf{c}(\mathbf{x}), \tag{2.2}$$

is used to transform the constrained optimization problem into a system of nonlinear equations, the first-order optimality conditions:

$$\begin{Bmatrix} \partial_x \mathcal{L} \\ \partial_\lambda \mathcal{L} \end{Bmatrix} (\mathbf{x}, \boldsymbol{\lambda}) = \begin{Bmatrix} \mathbf{g}(\mathbf{x}) + \mathbf{A}(\mathbf{x})^T \boldsymbol{\lambda} \\ \mathbf{c}(\mathbf{x}) \end{Bmatrix} = \mathbf{0} \quad (\text{or } \mathbf{h}(\mathbf{q}) = \mathbf{0}), \tag{2.3}$$

where $\mathbf{q} := \{\mathbf{x}, \boldsymbol{\lambda}\}^T$ represents the optimization variables and Lagrange multipliers. As in part I, $\mathbf{g}$ is the gradient of the objective function, $\mathbf{A}$ the Jacobian of the constraints, and $\mathbf{W}$ the Hessian of the Lagrangian. Consistent with part I, we think of $\mathbf{x}$, $\mathbf{g}$, $\mathbf{A}$, and $\mathbf{W}$ as being partitioned into state (indicated by an s subscript) and decision variable (d subscript) components. We use Newton's method to solve for $\mathbf{x}$ and $\boldsymbol{\lambda}$. A Newton step on the optimality conditions is given by

$$\begin{bmatrix} \mathbf{W} & \mathbf{A}^T \\ \mathbf{A} & \mathbf{0} \end{bmatrix} \begin{Bmatrix} \mathbf{p}_x \\ \mathbf{p}_\lambda \end{Bmatrix} = - \begin{Bmatrix} \mathbf{g} + \mathbf{A}^T\boldsymbol{\lambda} \\ \mathbf{c} \end{Bmatrix} \quad (\text{or } \mathbf{K}\mathbf{v} = -\mathbf{h}), \tag{2.4}$$

where $\mathbf{p}_x$ and $\mathbf{p}_\lambda$ are the updates of $\mathbf{x}$ and $\boldsymbol{\lambda}$ from the current to the next iteration. In part I we reviewed a popular algorithm for solving for a KKT point, RSQP and in particular its quasi-Newton variant (Algorithm 3 in part I). Although RSQP is efficient and robust, it often does not scale very well with the number of decision variables. It avoids solving (2.4) directly by reduction onto the decision space and in doing so requires repeated solution of linearized forward and adjoint problems. Thus, it can be very inefficient for large-scale PDE-constrained optimization. We argued that a better approach would be to remain in the full space of states, decisions, and multipliers by using a Krylov method to solve (2.4). For most problems, however, the KKT matrix is notoriously ill-conditioned. Motivated by this, part I proposed a family of efficient preconditioners. The key idea was to use an approximate RSQP method as a preconditioner. We showed that RSQP can be viewed as a block-LU factorization in which the reduced Hessian $\mathbf{W}_z$ is the Schur complement for the decision variables. It has the property that the only systems that have to be solved involve the reduced Hessian and the Jacobian of the state equations (and its transpose). Therefore, by using a limited memory quasi-Newton approximation of the reduced Hessian, and by replacing the linearized PDE solves by applications of their preconditioners, we obtain a method that requires no PDE solves within a Krylov iteration, yet maintains Newton convergence in the outer iteration. A sketch of the LNKS method for solving the KKT system (2.4) is given by Algorithm 1, in which $\mathbf{P}^{-1}$ is an application of the approximate RSQP preconditioner.

Algorithm 1. Lagrange–Newton–Krylov–Schur (LNKS).

```
1: Choose $\mathbf{x}$, $\boldsymbol{\lambda}$
2: loop
3:    Check for convergence
4:    Compute $\mathbf{c}$, $\mathbf{g}$, $\mathbf{A}$, $\mathbf{W}$
5:    Solve $\mathbf{P}^{-1}\mathbf{K}\mathbf{v} = \mathbf{P}^{-1}\mathbf{h}$                    (Newton step)
6:    Update $\mathbf{x} = \mathbf{x} + \mathbf{p}_x$
7:    Update $\boldsymbol{\lambda} = \boldsymbol{\lambda} + \mathbf{p}_\lambda$
8: end loop
```

Nevertheless, there are two issues that should be addressed before we can claim a fast and robust general-purpose algorithm. The first is whether the LNKS algorithm can be made convergent for any initial guess $(\mathbf{x}_0, \boldsymbol{\lambda}_0)$, and the second is whether we can utilize inexactness in the inner iterations to further accelerate LNKS. Within this framework we examine line search algorithms, reverting to a QN-RSQP step when a LNKS steps fails to make progress, continuation, and inexact Newton methods.

2.1. Line search methods. Algorithm 1 is only locally convergent. Popular methods to globalize Newton's method include line search and trust region algorithms. Details can be found in [21]. Trust region methods, especially in combination with RSQP and inexact Newton methods, have been extended successfully to PDE-constrained optimization [14, 17, 19]. Global convergence proofs for these methods can be found in [5]. Trust region methods are often based on the Steihaug modification of the conjugate gradient (CG) algorithm [24]. However, this approach works well only with positive definite systems. It is not obvious how to use trust regions with an indefinite Krylov solver (which is required for the KKT system) and thus we have opted for a line search algorithm to help globalize LNKS.

An important component of a line search algorithm is the choice of a merit function: a scalar function (of the optimization variables) that monitors the progress of the algorithm. In contrast with unconstrained optimization, the choice of a merit function is not straightforward, since we are trying to balance minimization of the objective function with feasibility of the constraints. Two common choices are the l_1 merit function,

$$\phi(\mathbf{x}) := f + \rho_\phi \|\mathbf{c}\|_1, \tag{2.5}$$

and the augmented Lagrangian merit function,

$$\phi(\mathbf{x}, \boldsymbol{\lambda}) := f + \mathbf{c}^T \boldsymbol{\lambda} + \frac{\rho_\phi}{2} \mathbf{c}^T \mathbf{c}. \tag{2.6}$$

The scalar ρ_ϕ is the *penalty parameter*—a weight chosen to balance minimization of the objective function with minimization of the residuals of the constraints. Both functions are "exact" provided the penalty parameter is large enough. By *exact* we mean that if $\mathbf{x}^*$ is a minimizer for (2.1), then it is also an (unconstrained) minimizer for the merit function. A crucial property of a merit function is that it should accept unit step lengths close to a solution in order to allow full Newton steps and thus quadratic convergence. The l_1 merit function suffers from the "Maratos" effect; that is, sometimes it rejects good steps and slows down the algorithm. The augmented Lagrangian merit function does not exhibit such behavior but its drawback is that it requires accurate estimates of the Lagrange multipliers.

The outline of a general line search method is given in Algorithm 2. To simplify notation we use $\phi(\alpha)$ for $\phi(\mathbf{q} + \alpha \mathbf{v})$ and $\phi(0)$ for $\phi(\mathbf{q})$, and likewise for the derivative $\nabla\phi$. The algorithm used to compute the search direction $\mathbf{v}$ is intentionally left unspecified. All that matter to ensure global convergence are the properties of the merit function and the properties of $\mathbf{v}$. Step 3 in Algorithm 2 lists three conditions on $\mathbf{v}$: descent direction, sufficient angle, and sufficient step length size [9]. The condition in step 4 is often called the Armijo condition. If ϕ is bounded and has a minimum, and if $\mathbf{v}$ is bounded, Algorithm 2 is guaranteed to converge to a local minimum [20]. We use a simple backtracking line search, with a factor α of 0.5. The search is bounded so that $\alpha_{\min} \leq \alpha \leq 1$. As mentioned before, the choice of the penalty parameter has a great effect on the performance of the algorithm.

For a step computed by quasi-Newton RSQP (Algorithm 3 of part I), the update for the l_1-merit function is relatively straightforward. The directional derivative for a search direction $\mathbf{p}_x$ is given by

$$\nabla\phi^T \mathbf{p}_x = \mathbf{g}^T \mathbf{p}_x - \rho_\phi \|\mathbf{c}\|_1. \tag{2.7}$$

If $\mathbf{W}_z$ is positive definite, it can be shown that by setting

$$\rho_\phi = \|\boldsymbol{\lambda}\|_\infty + \delta, \quad \delta > 0, \tag{2.8}$$

Algorithm 2. Line search.

```
1: Choose $\mathbf{q}$, $\delta_A > 0$ and $\kappa_1$, $\kappa_2$ arbitrary constants (strictly positive)
2: while Not converged do
3:    Compute search direction $\mathbf{v}$ so that
          $\mathbf{v}^T \nabla\phi(0) < 0$
          $|\mathbf{v}^T \nabla\phi(0)| \geq \kappa_1 \, \|\mathbf{v}\| \, \|\nabla\phi(0)\|$          angle condition
          $\|\mathbf{v}\| \geq \kappa_2 \|\nabla\phi(0)\|$          length condition
4:    Compute $\alpha$ such that $\phi(\alpha) \leq \phi(0) + \alpha\delta_A \mathbf{v}^T \nabla\phi(0)$          Armijo condition
5:    Set $\mathbf{q} = \mathbf{q} + \alpha\mathbf{v}$
6: end while
```

we obtain a descent direction. In our numerical experiments we have used the l_1-merit function with QN-RSQP and the augmented Lagrangian with LNKS. The l_1-merit function performed reasonably well. However, we did observe the Maratos effect. To overcome this obstacle we have implemented a second-order correction, in which an extra normal step toward feasibility is taken [21, p. 570].

When an augmented Lagrangian merit function is used, the penalty parameter should be chosen differently. The directional derivative of the augmented Lagrangian merit function is given by

$$\nabla\phi^T \mathbf{v} = (\mathbf{g} + \mathbf{A}^T \boldsymbol{\lambda} + \rho_\phi \mathbf{A}^T \mathbf{c})^T \mathbf{p}_x + \mathbf{c}^T \mathbf{p}_\lambda. \tag{2.9}$$

Lagrange multipliers slightly complicate the algorithm since we have to compute $\mathbf{p}_\lambda$. $\boldsymbol{\lambda}$ may be considered a function of $\mathbf{x}$ [4, 8] or an independent variable [5, 23] or may be simply ignored by setting $\mathbf{p}_\lambda = 0$ [25]. In LNKS we solve for $\boldsymbol{\lambda}$ simultaneously with $\mathbf{x}$ and it is natural to use the step $\mathbf{p}_\lambda$. On the other hand, RSQP uses $\boldsymbol{\lambda} = -\mathbf{A}_s^{-T}\mathbf{g}_s$ and it seems natural to consider $\boldsymbol{\lambda}$ a function of $\mathbf{x}$. In this case the last term in (2.9) is given by

$$\mathbf{c}^T \mathbf{p}_\lambda = \mathbf{c}^T (\partial_x \boldsymbol{\lambda}) \mathbf{p}_x,$$

where

$$\partial_x \boldsymbol{\lambda} := -\mathbf{A}_s^{-T} [\mathbf{W}_{ss} \; \mathbf{W}_{sd}].$$

(However, this formula cannot be used with the QN-RSQP method of Algorithm 3, part I, since second derivatives are not computed.) If we set

$$\rho_\phi = \frac{(\mathbf{g} + \mathbf{A}^T \boldsymbol{\lambda})\mathbf{p}_x + \mathbf{c}^T \mathbf{p}_\lambda + \delta}{\mathbf{c}^T \mathbf{A} \mathbf{p}_x}, \quad \delta > 0, \tag{2.10}$$

we obtain a descent direction.

2.2. Combining QN-RSQP with LNKS. For iterates far from the solution, relying solely on a line search algorithm to globalize LNKS is not sufficient, since the Newton step is likely to be of poor quality. Usually global convergence can be shown if the reduced (and not full) Hessian $\mathbf{W}_z$ is positive definite. If $\mathbf{W}_z$ is positive definite (and assuming the system (2.4) is solved exactly), then the resulting step $\mathbf{v}$ satisfies the Armijo sufficient decrease criterion. Far from the minimum, however, $\mathbf{W}_z$ can be singular or indefinite. On the other hand, certain quasi-Newton methods, like BFGS, are preferable for iterates far from the solution since they can guarantee positive definiteness. For this reason (and for preconditioning purposes) LNKS does maintain a BFGS approximation for $\mathbf{W}_z$: if a computed Newton search direction fails to satisfy the Armijo criterion, we discard it and revert to a QN-RSQP step.

2.3. Continuation. One of the standard assumptions in global convergence proofs is the full rank of the constraint Jacobian for all iterates. In LNKS, this translates to the nonsingularity of the state Jacobian $\mathbf{A}_s$, i.e., the PDE state operator. For highly nonlinear PDEs such as the Navier–Stokes equations, this can be an unrealistic assumption. Even if $\mathbf{A}_s$ is nonsingular, severe ill-conditioning may cause both QN-RSQP and LNKS algorithms to stall. Indeed, in our numerical experiments, the most difficult computation (for iterates far from the solution) was converging the $\mathbf{A}_s$-related linear solves. Krylov solvers often reached their maximum iteration counts without a significant decrease in the linear system residual. As a result, the iterates were of poor quality and the algorithm stagnated as it was impossible to compute a search direction, be it from QN-RSQP or LNKS.

One remedy for this problem is parameter continuation. This idea (in its simplest form) works when we can express the nonlinearity of the problem as a function of a single scalar parameter. Continuation is suitable for problems in which the underlying PDE has a parameter that scales (and thus determines the effects of) nonlinear terms. Examples of such parameters are the Reynolds number for viscous flow, the Mach number for compressible flow, the Weissenberg number for viscoelastic flow, load magnitude for buckling problems, and the Hartman number in magnetohydrodynamics. In problems where such a parameter cannot be found, an alternative approach is to use a pseudotransient continuation scheme [18], a homotopy method [1], or mesh-size continuation.

Continuation allows uphill steps to be taken (unlike monotone line search methods) and generates good initial guesses, not only for the optimization variables, but also for the penalty parameter in the merit function. An important feature of the continuation algorithm is that under certain conditions it globalizes trivially.[1] If the continuation step places the next iterate outside the attraction basin of the Newton method, then we simply reduce the continuation step size. In principle, the method globalizes LNKS without the need to use line search or some other globalization strategy. Nevertheless, taking a large number of continuation steps significantly slows down the algorithm. Experience from our numerical experiments suggests that the best strategy for globalizing LNKS is a combination of line searching, reverting to quasi-Newton steps, and continuation.

2.4. Inexact Newton method. Before we discuss the inexact Newton method in the context of LNKS, we briefly summarize a few results for a general nonlinear system of equations. Assume we want to solve $\mathbf{h}(\mathbf{q}) = \mathbf{0}$. Further assume the following: (1) $\mathbf{h}$ and $\mathbf{K} := \partial_q \mathbf{h}$ are sufficiently smooth in a neighborhood of a solution $\mathbf{q}^*$; (2) at each iteration an inexact Newton method computes a step $\mathbf{v}$ that satisfies

$$\|\mathbf{K}\mathbf{v} + \mathbf{h}\| \leq \eta_N \|\mathbf{h}\|, \tag{2.11}$$

where η_N is often called the *forcing term*. It can be shown that if $\eta_N < 1$, then $\mathbf{q} \to \mathbf{q}^*$ linearly; if $\eta_N \to 0$, then $\mathbf{q} \to \mathbf{q}^*$ superlinearly; and if $\eta_N = \mathcal{O}(\|\mathbf{h}\|)$, then we recover the quadratic convergence rate of an exact Newton method. The forcing term is usually given by

$$\eta_N = \frac{\|\mathbf{h}_{(+)} - \mathbf{h} - \mathbf{K}\mathbf{v}\|}{\|\mathbf{h}\|}. \tag{2.12}$$

Other alternatives exist (for details see [7]).

[1]This is true only when the initial problem is a well-posed quadratic programming problem (like Stokes) and all iterates on the continuation path are far from turning and bifurcation points.

The extension of inexact Newton methods to unconstrained optimization problems is relatively easy. The extension becomes more complicated for problems with constraints. In [14] global convergence proofs are given for a trust region RSQP-based algorithm, but to our knowledge such an approach has not been extended to full space algorithms. Close to a KKT point the theory for Newton's method applies and one can use the analysis presented in [6] to show that the inexact version of the LNKS algorithm converges. However, the line search we are using is not based on the residual of the KKT equations but instead on the merit function discussed in the previous session. It is not obvious that an inexact Newton step (which simply reduces $\|\mathbf{h}\|$) will satisfy the merit function criteria. *We will show for points that are close enough to the solution, inexact Newton steps do satisfy the Armijo criterion for the merit function line search.* Our analysis is based on the augmented Lagrangian merit function.[2] We assume that, locally, $\mathbf{A}$ and $\mathbf{K}$ are nonsingular and uniformly bounded. We define $\kappa_1 := \max \|\mathbf{K}^{-1}(\mathbf{q})\|$ for $\mathbf{q}$ in the neighborhood of the solution $\mathbf{q}^*$. We also define $\mathbf{v}$ as the exact solution of the (linearized) KKT system so that

$$\mathbf{K}\mathbf{v} + \mathbf{h} = \mathbf{0}, \tag{2.13}$$

and $\tilde{\mathbf{v}}$ the approximate solution so that

$$\mathbf{K}\tilde{\mathbf{v}} + \mathbf{h} = \mathbf{r}. \tag{2.14}$$

We also have $\|\mathbf{r}\| = \eta\|\mathbf{h}\|$, $0 < \eta \leq \eta_N$, from the inexact Newton stopping criterion (2.11). By (2.3) we get that $\|\mathbf{h}\|^2 = \|\mathbf{g} + \mathbf{A}^T\boldsymbol{\lambda}\|^2 + \|\mathbf{c}\|^2$ and since $\mathbf{A}$ is uniformly bounded, there is constant κ_2 such that

$$\|\mathbf{A}^T\mathbf{c}\| \leq \kappa_2\|\mathbf{h}\|. \tag{2.15}$$

Besides the assumptions on $\mathbf{K}$ and $\mathbf{A}$ we also assume the following: (1) ρ_ϕ is sufficiently large so that the merit function is exact and $\|\nabla\phi\| \geq \kappa_3\|\mathbf{h}\|$ for some constant κ_3; (2) $\mathbf{v}$ is a descent direction and satisfies the angle and length conditions as well as the Armijo condition. From the latter it is immediate that $\mathbf{v}$ satisfies the Cauchy fraction condition:[3]

$$|\nabla\phi^T\mathbf{v}| \geq 2\kappa_4\|\nabla\phi\|^2. \tag{2.16}$$

We will show that if η is small enough, then the approximate step $\tilde{\mathbf{v}}$ satisfies the Cauchy fraction, angle, and length conditions. Then, we will use a theorem from [20] to conclude that the Armijo condition is satisfied with unit step lengths. Therefore if $\eta = \mathcal{O}(\|\mathbf{h}\|)$, quadratic convergence is preserved.

From (2.13) and (2.14) we have

$$\nabla\phi^T\tilde{\mathbf{v}} = \nabla\phi^T\mathbf{v} + \nabla\phi^T\mathbf{K}^{-1}\mathbf{r},$$

and thus by (2.16) we get

$$|\nabla\phi^T\tilde{\mathbf{v}}| \geq 2\kappa_4\|\nabla\phi\|^2 - |\nabla\phi^T\mathbf{K}^{-1}\mathbf{r}|.$$

Therefore, to satisfy the Cauchy fraction condition

$$|\nabla\phi^T\tilde{\mathbf{v}}| \geq \kappa_4\|\nabla\phi\|^2, \tag{2.17}$$

[2]For brevity we drop the subscript from ϕ_L and just use the symbol ϕ for the augmented Lagrangian merit function.

[3]The Cauchy step is a steepest descent step for the merit function.

we need to show that

$$|\nabla\phi^T \mathbf{K}^{-1}\mathbf{r}| \leq \kappa_4 \|\nabla\phi\|^2. \tag{2.18}$$

The gradient of the merit function is given by

$$\nabla\phi = \mathbf{h} + \rho_\phi \begin{Bmatrix} \mathbf{A}^T\mathbf{c} \\ \mathbf{0} \end{Bmatrix},$$

and thus

$$\begin{aligned} |\nabla\phi^T \mathbf{K}^{-1}\mathbf{r}| &= \left| \mathbf{h}^T\mathbf{K}^{-1}\mathbf{r} + \rho_\phi \begin{Bmatrix} \mathbf{A}^T\mathbf{c} \\ \mathbf{0} \end{Bmatrix}^T \mathbf{K}^{-1}\mathbf{r} \right| \\ &\leq \kappa_1(\|\mathbf{h}\|\,\|\mathbf{r}\| + \rho_\phi\|\mathbf{A}^T\mathbf{c}\|\,\|\mathbf{r}\|) \\ &\leq \kappa_1\eta(\|\mathbf{h}\|^2 + \rho_\phi\|\mathbf{A}^T\mathbf{c}\|\,\|\mathbf{h}\|) \\ &\leq \kappa_1\eta(1+\rho_\phi\kappa_2)\|\mathbf{h}\|^2 \\ &\leq \kappa_1\eta(1+\rho_\phi\kappa_2)\frac{\|\nabla\phi\|^2}{\kappa_3^2}. \end{aligned}$$

If

$$\eta \leq \frac{\kappa_4\ \kappa_3^2}{\kappa_1(1+\rho_\phi\kappa_2)}, \tag{2.19}$$

then (2.18) holds. If we choose a superlinearly convergent inexact Newton variant, then

$$\eta \leq \eta_N \to 0,$$

and therefore, close to the solution (2.19) holds. We also have that

$$\begin{aligned} \tilde{\mathbf{v}} &= \mathbf{K}^{-1}(\mathbf{r}-\mathbf{h}), \\ \|\tilde{\mathbf{v}}\| &\leq \kappa_1(1+\eta)\|\mathbf{h}\|, \\ \|\tilde{\mathbf{v}}\| &\leq \kappa_1(1+\eta)\frac{\|\nabla\phi\|}{\kappa_3}, \\ \|\tilde{\mathbf{v}}\| &\leq \kappa_5\|\nabla\phi\|. \end{aligned} \tag{2.20}$$

By combining (2.20) and (2.17) we get

$$|\nabla\phi^T\tilde{\mathbf{v}}| \geq \kappa_4\|\nabla\phi\|^2 \geq \kappa_4\kappa_5\|\nabla\phi\|\,\|\tilde{\mathbf{v}}\|$$

and

$$\|\nabla\phi\|\,\|\tilde{\mathbf{v}}\| \geq \kappa_6|\nabla\phi^T\tilde{\mathbf{v}}| \geq \kappa_6\kappa_4\|\nabla\phi\|^2 \Longrightarrow \|\tilde{\mathbf{v}}\| \geq \kappa_7\|\nabla\phi\|.$$

That is, the length and angle conditions are satisfied. It can be shown [20, Theorem 10.6] that there is an α, bounded below, so that the Armijo condition holds true. Thus by choosing δ_A small enough, the Armijo condition is satisfied with unit step length. Hence the quadratic convergence rate associated with Newton's method is observed; i.e., the inexactness does not interfere with the merit function. In addition it can be shown that the augmented Lagrangian merit function allows unit step length near the solution (see [8, 23] and the references therein). Finally, notice that convergence does not require that $\eta_N \to 0$; it only requires that η_N is small enough. This is in contrast with inexact reduced space methods which require the tolerances to become tighter as the iterates approach the solution [14].

2.5. The globalized inexact LNKS algorithm. In this section we present the complete LNKS method incorporating the globalization and inexactness strategies discussed above, and give a high-level description of implementation details and specific heuristics used to accelerate convergence. The basic steps of our method are given in Algorithm 3.

Algorithm 3. Globalized LNKS.

```
1:  Choose $\mathbf{x}_s$, $\mathbf{x}_d$, $\rho_\phi$, $\delta_A$, set Re = Re$_{start}$, tol = tol$_0$
2:  $\mathbf{A}_s^T\boldsymbol{\lambda} + \mathbf{g}_s \approx \mathbf{0}$                                solve inexactly for $\boldsymbol{\lambda}$
3:  while Re $\neq$ Re$_{target}$ do
4:    loop
5:      Evaluate $f$, $\mathbf{c}$, $\mathbf{g}$, $\mathbf{A}$, $\mathbf{W}$
6:      $\mathbf{g}_z = \mathbf{g}_d + \mathbf{A}_d^T\boldsymbol{\lambda}$
7:      Check convergence: $\|\mathbf{h}\| \leq$ tol
8:      $\mathbf{P}^{-1}\mathbf{K}\mathbf{v} + \mathbf{P}^{-1}\mathbf{h} \approx \mathbf{0}$                          solve inexactly for $\mathbf{v}$
9:      Compute $\rho_\phi$ such that $\nabla\phi^T(0)\mathbf{v} \leq 0$
10:     Compute $\alpha$ s.t. $\phi(\alpha) \leq \phi(0) + \delta_A\alpha(\nabla\phi^T(0)\mathbf{v})$
11:     if Line search failed then
12:       Compute $\alpha$ s.t. $\|\mathbf{h}(\alpha)\| < (1 - \delta_A\alpha\,(\mathbf{v}^T\,\mathbf{K}\,\mathbf{h}(0)))$  Armijo for KKT residual
13:     end if
14:     if LNKS step failed then
15:       $\mathbf{B}_z\mathbf{p}_d = -\mathbf{g}_z$                                   solve inexactly for $\mathbf{p}_d$
16:       $\mathbf{A}_s\mathbf{p}_s + \mathbf{A}_d\mathbf{p}_d + \mathbf{c} \approx \mathbf{0}$                        solve inexactly for $\mathbf{p}_s$
17:       $\mathbf{A}_s^T\boldsymbol{\lambda}_+ + \mathbf{g}_s \approx \mathbf{0}$                           solve inexactly for $\boldsymbol{\lambda}_+$
18:       Compute $\alpha$ s.t. $\phi(\alpha) \leq \phi(0) + \delta_A\alpha(\nabla\phi^T(0)\mathbf{v})$
19:       if Line search on QN-RSQP step failed then
20:         Reduce Re and go to step 5.
21:       end if
22:     end if
23:     $\boldsymbol{\lambda}_+ = \boldsymbol{\lambda} + \mathbf{p}_\lambda$                                  (only for LNKS step)
24:     $\mathbf{x}_+ = \mathbf{x} + \mathbf{p}_x$
25:   end loop
26:   Re = Re + $\Delta$ Re
27:   Tighten tol
28: end while
```

The algorithm uses a three-level iteration.

- In the *continuation iteration* (lines 3–28) the continuation parameter is gradually increased until the target value is reached.
- The *outer iteration* (lines 4–25) corresponds to the Lagrange–Newton solver for the KKT optimality system for a fixed continuation number.
- The *inner iteration* (line 8 for LNKS, and lines 15–17 for QN-RSQP) refers to the solution of the linearized KKT system.

The outer iteration consists of two core branches: the computation of the LNKS search direction and the computation of a search direction with the limited-memory BFGS QN-RSQP method. The default branch is the LNKS step. If this step fails to satisfy the line search conditions, we switch to QN-RSQP. If the QN-RSQP search direction fails to satisfy the line search criteria as well, then we reduce the continuation parameter Re and return to the beginning of the continuation loop (line 3).

There are several possible instantiations of this framework. Below, we give some additional implementation details on our algorithmic choices.

- The linear solves in lines 8, 16, and 17 are performed inexactly. We follow [7] in choosing the forcing term. For the LNKS step (line 8) we use $\|\mathbf{h}\|$ as the residual that drives the Newton solver; for the QN-RSQP step (lines 15–18) we use $\|\mathbf{c}\|$ and $\|\mathbf{g}_z\|$.
- We allow for nonmonotone line searches. If the LNKS step (line 8) is rejected by the merit function line search (line 10) we do not switch immediately to QN-RSQP. Instead we do a line search on the KKT residual (line 12) and if the step is accepted we use it to update the variables for the next iteration. However, we do store information ($\boldsymbol{\lambda}$ and $\mathbf{x}$, the merit function value and gradient) for the iterate for which the LNKS step failed, and we insist that a subsequent iterate satisfies the conditions of the merit line search (evaluated at the failure point) after a fixed number of iterations. Typically, we permit two iterations before we demand reduction of the merit function. If the Armijo criterion is still violated, we backtrack to the original point of failure and switch to a QN-RSQP method (lines 15–18).
- We use various heuristics to bound the penalty parameter and possibly reduce it. A new penalty parameter ρ_ϕ^+ is computed using the LNKS step and formula (2.10). If $\rho_\phi^+ > 4\rho_\phi$ we update the penalty parameter and switch to QN-RSQP. If $\rho_\phi^+ < \rho_\phi/4$ we *reduce* the penalty parameter and set $\rho_\phi^+ = 0.5\rho_\phi$. We also reduce the penalty parameter if there is a successful search on the KKT residual (step 12).
- A Lanczos algorithm can be used to (approximately) check the second-order optimality conditions. If an extremal eigenvalue of $\tilde{\mathbf{W}}_z$ is negative, then we abandon the full space and revert to a QN-RSQP step. The eigenvalue computation is frozen through a single continuation step, but if a negative direction is detected, they are recomputed at each SQP iteration.
- In line 6 we use the adjoint variables to update the reduced gradient. This is equivalent to $\mathbf{g}_z = \mathbf{g}_d - \mathbf{A}_d^T \mathbf{A}_s^{-T} \mathbf{g}_s$ if $\boldsymbol{\lambda}$ is computed by solving exactly $\mathbf{A}_s^T \boldsymbol{\lambda} + \mathbf{g}_s = \mathbf{0}$. When $\boldsymbol{\lambda}$ is taken from the LNKS step computation, it includes second-order terms (which tend to zero as we approach a stationary point). This introduces error in the computation of $\mathbf{g}_z$. When $\boldsymbol{\lambda}$ is taken from QN-RSQP it introduces additional error since we never solve the linear systems exactly.
- Typical values for the parameters are $\rho_\phi = 0.5$, $\delta_A = 10^{-4}$, and tol $= 10^{-5}\|\mathbf{h}_0\|$ (following [6]). Here $\mathbf{h}_0$ is the value of the KKT residual at the first iteration of each outer loop.

We have shown how it is possible to augment the basic LNKS method with line search and continuation, safeguard it with QN-RSQP steps, and further accelerate it with inexact Newton. We have shown that inexactness does not interfere with the line search algorithm, and we have described the globalized algorithm and various heuristics that are observed to improve performance.

In the next section we study an optimal control problem for the steady incompressible Navier–Stokes equations. We cite results on the existence and uniqueness of solutions and make comparisons between the discrete and continuous forms of the optimality conditions.

3. Formulation of an optimal control problem.

We turn our attention to the formulation and well-posedness of a specific optimization problem: the Dirichlet control of the steady incompressible Navier–Stokes equations. We present the continuous form of the KKT optimality conditions and we cite convergence results for finite element approximations from [15] and [16]. A survey and articles on this topic can be found in [11]. More on the Navier–Stokes equations can be found in [10, 13].

We study problems in which we specify both Dirichlet and Neumann boundary conditions. The controls are restricted to be of Dirichlet type only, but the theory is similar for distributed and Neumann controls [15].

3.1. Continuous optimality conditions. We use the velocity-pressure $(\boldsymbol{u}, p)$ form of the incompressible steady Navier–Stokes equations. We begin by writing the following strong form of the flow equations:

$$\begin{aligned}
-\nu\nabla\cdot(\nabla\boldsymbol{u}+\nabla\boldsymbol{u}^T)+(\nabla\boldsymbol{u})\boldsymbol{u}+\nabla p=\boldsymbol{b} \quad &\text{in } \Omega,\\
\nabla\cdot\boldsymbol{u}=0 \quad &\text{in } \Omega,\\
\boldsymbol{u}=\boldsymbol{u}_g \quad &\text{on } \Gamma_u,\\
\boldsymbol{u}=\boldsymbol{u}_d \quad &\text{on } \Gamma_d,\\
-p\boldsymbol{n}+\nu(\nabla\boldsymbol{u}+\nabla\boldsymbol{u}^T)\boldsymbol{n}=\boldsymbol{0} \quad &\text{on } \Gamma_N.
\end{aligned} \tag{3.1}$$

Here $\nu = 1/\mathrm{Re}$ and the decision variables are the control velocities $\mathbf{u}_d$ on Γ_d. For a forward solve we need not distinguish between Γ_d and Γ_u. In the optimization problem, however, $\boldsymbol{u}_d$ is not known. We will present a mixed formulation that treats the tractions on the Dirichlet boundary Γ_d as additional unknown variables. The traction variables play the role of Lagrange multipliers (not to be confused with the Lagrange multipliers of the optimal control problem) and are used to enforce the Dirichlet boundary conditions [2].

By $L^2(\Omega)$ we denote the space of scalar functions that are square-integrable in Ω, and by $\boldsymbol{H}^1(\Omega)$ we denote the space of vector functions whose first derivatives are in $\boldsymbol{L}^2(\Omega)$. $\boldsymbol{H}^{1/2}(\Gamma)$ is the trace space (the restriction on Γ) of functions belonging to $\boldsymbol{H}^1(\Omega)$. Finally $\boldsymbol{H}^{-k}(D)$ is the set of bounded linear functionals on functions belonging to $\boldsymbol{H}^k(D)$, where D is some smooth domain in $\mathbb{R}^3$. We also define $\boldsymbol{V} := \{\boldsymbol{v} \in \boldsymbol{H}^1(\Omega) : \boldsymbol{v}|_{\Gamma_u} = \boldsymbol{0}\}$. We define the following bilinear and trilinear forms associated with the Navier–Stokes equations:

$$\begin{aligned}
a(\boldsymbol{u},\boldsymbol{v}) &:= \int_\Omega (\nabla\boldsymbol{u}+\nabla\boldsymbol{u}^T)\cdot(\nabla\boldsymbol{v}+\nabla\boldsymbol{v}^T)\,d\Omega \quad \forall \boldsymbol{u},\boldsymbol{v}\in\boldsymbol{H}^1(\Omega),\\
c(\boldsymbol{w},\boldsymbol{u},\boldsymbol{v}) &:= \int_\Omega (\nabla\boldsymbol{u})\boldsymbol{w}\cdot\boldsymbol{v}\,d\Omega \quad \forall \boldsymbol{u},\boldsymbol{v},\boldsymbol{w}\in\boldsymbol{H}^1(\Omega),\\
b(q,\boldsymbol{v}) &:= \int_\Omega -q\nabla\cdot\boldsymbol{v}\,d\Omega \quad \forall q\in L^2,\ \boldsymbol{v}\in\boldsymbol{H}^1(\Omega).
\end{aligned}$$

We also use the notation $(\boldsymbol{x},\boldsymbol{y})_D$ for $\int_D \boldsymbol{x}\cdot\boldsymbol{y}\,dD$.

In the weak formulation of (3.1) we seek $\boldsymbol{u} \in \boldsymbol{H}^1(\Omega)$, $p \in L^2(\Omega)$, and $\boldsymbol{\sigma} \in H^{-1/2}(\Gamma_d)$ such that

$$\begin{aligned}
\nu a(\boldsymbol{u},\boldsymbol{v})+c(\boldsymbol{u},\boldsymbol{u},\boldsymbol{v})+b(p,\boldsymbol{v})-(\boldsymbol{\sigma},\boldsymbol{v})_{\Gamma_d}=(\boldsymbol{f},\boldsymbol{v})_\Omega \quad &\forall\boldsymbol{v}\in\boldsymbol{V},\\
b(q,\boldsymbol{u})=0 \quad &\forall q\in L^2(\Omega),\\
-(\boldsymbol{t},\boldsymbol{u})_{\Gamma_d}=-(\boldsymbol{t},\boldsymbol{u}_d)_{\Gamma_d} \quad &\forall\boldsymbol{t}\in\boldsymbol{H}^{-1/2}(\Gamma_d).
\end{aligned} \tag{3.2}$$

We also define $\boldsymbol{d}$ to be the decision field (so that $\boldsymbol{u}_d = \boldsymbol{d}$). Based on the above formulation we proceed in defining the Lagrangian function for the optimization problem. The objective function is given by

$$\mathcal{J}(\boldsymbol{u},\boldsymbol{d}) := \frac{\nu}{2}a(\boldsymbol{u},\boldsymbol{u})+\frac{\rho}{2}(\boldsymbol{d},\boldsymbol{d})_{\Gamma_d}, \tag{3.3}$$

and (the weak form of) the constraints are given by (3.2). We define the Lagrangian function $\mathcal{L}$ by

$$\begin{aligned}
&\mathcal{L}(\boldsymbol{u}, p, \boldsymbol{d}, \boldsymbol{\sigma}, \boldsymbol{\lambda}, \mu, \boldsymbol{\tau}) := \mathcal{J}(\boldsymbol{u}, \boldsymbol{d}) \\
&\qquad + \nu a(\boldsymbol{u}, \boldsymbol{\lambda}) + c(\boldsymbol{u}, \boldsymbol{u}, \boldsymbol{\lambda}) - (\boldsymbol{\sigma}, \boldsymbol{\lambda})_{\Gamma_d} - (\boldsymbol{f}, \boldsymbol{\lambda})_{\Omega} + b(p, \boldsymbol{\lambda}) \\
&\qquad + b(\mu, \boldsymbol{u}) - (\boldsymbol{\tau}, \boldsymbol{u} - \boldsymbol{d})_{\Gamma_d} \\
&\qquad\qquad \forall \boldsymbol{u} \in \boldsymbol{H}^1(\Omega), \quad p \in L^2(\Omega), \quad \boldsymbol{\sigma} \in \boldsymbol{H}^{-1/2}(\Gamma_d), \quad \boldsymbol{d} \in \boldsymbol{H}^{1/2}(\Gamma_d), \\
&\qquad\qquad \forall \boldsymbol{\lambda} \in \boldsymbol{V}, \quad \mu \in L^2(\Omega), \quad \boldsymbol{\tau} \in \boldsymbol{H}^{-1/2}(\Gamma_d).
\end{aligned} \tag{3.4}$$

Here $\boldsymbol{\lambda}$, μ, $\boldsymbol{\tau}$ are the Lagrange multipliers for the state variables $\boldsymbol{u}$, p, $\boldsymbol{\sigma}$. By taking variations with respect to the Lagrange multipliers we obtain (3.2) augmented with $\boldsymbol{u}_d = \boldsymbol{d}$ on Γ_d. Taking variations with respect to the states $\boldsymbol{u}$, p, $\boldsymbol{\sigma}$ we obtain the weak form of the adjoint equations

$$\begin{aligned}
&\nu a(\boldsymbol{v}, \boldsymbol{\lambda}) + c(\boldsymbol{v}, \boldsymbol{u}, \boldsymbol{\lambda}) + c(\boldsymbol{u}, \boldsymbol{v}, \boldsymbol{\lambda}) + b(\mu, \boldsymbol{v}) + (\boldsymbol{\tau}, \boldsymbol{v})_{\Gamma_d} = -\nu a(\boldsymbol{u}, \boldsymbol{v}) \quad \forall \boldsymbol{v} \in \boldsymbol{V}, \\
&b(q, \boldsymbol{\lambda}) = 0 \quad \forall q \in L^2(\Omega), \\
&(\boldsymbol{t}, \boldsymbol{\lambda})_{\Gamma_d} = 0 \quad \forall \boldsymbol{t} \in \boldsymbol{H}^{-1/2}(\Gamma_d).
\end{aligned} \tag{3.5}$$

Finally, by taking variations with respect to $\boldsymbol{d}$ we obtain the decision equation

$$\rho(\boldsymbol{d}, \boldsymbol{r})_{\Gamma_d} + (\boldsymbol{\tau}, \boldsymbol{r})_{\Gamma_d} = 0 \quad \forall \boldsymbol{r} \in \boldsymbol{H}^{1/2}(\Gamma_d). \tag{3.6}$$

Equations (3.2), (3.5), (3.6) are the weak form of the first-order optimality conditions. Extensive discussion on the existence of a solution and the existence of the Lagrange multipliers can be found in [15, 16]. In [15] the existence of a local minimum for the optimization problem and the existence of Lagrange multipliers that satisfy the first-order optimality conditions are asserted.[4] Furthermore, uniqueness is shown for sufficiently small data. Note that in the absence of a Neumann condition ($\Gamma_N = \emptyset$) the controls have to satisfy the incompressibility condition $(\boldsymbol{d} \cdot \boldsymbol{n})_{\Gamma_d} = 0$.

The strong form of the adjoint and decision equations can be obtained by using the following integration by parts formulas:

$$\begin{aligned}
a(\boldsymbol{u}, \boldsymbol{v}) &= -(\boldsymbol{v}, \Delta \boldsymbol{u})_{\Omega} + ((\nabla \boldsymbol{u})\boldsymbol{n}, \boldsymbol{v})_{\Gamma}, \\
c(\boldsymbol{u}, \boldsymbol{v}, \boldsymbol{\lambda}) &= -c(\boldsymbol{u}, \boldsymbol{\lambda}, \boldsymbol{v}) - ((\nabla \cdot \boldsymbol{u})\boldsymbol{\lambda}, \boldsymbol{v})_{\Omega} + ((\boldsymbol{u} \cdot \boldsymbol{n})\boldsymbol{\lambda}, \boldsymbol{v})_{\Gamma}, \\
b(\mu, \boldsymbol{v}) &= (\nabla \mu, \boldsymbol{v})_{\Omega} - (\mu \boldsymbol{n}, \boldsymbol{v})_{\Gamma}.
\end{aligned}$$

Upon sufficient smoothness we arrive at the strong form of the optimality conditions. Equation (3.1) is the strong form of the constraints. The strong form of the adjoint equations is given by

$$\begin{aligned}
-\nu \nabla \cdot (\nabla \boldsymbol{\lambda} + \nabla \boldsymbol{\lambda}^T) + (\nabla \boldsymbol{u})^T \boldsymbol{\lambda} - (\nabla \boldsymbol{\lambda})\boldsymbol{u} + \nabla \mu = \nu \nabla \cdot (\nabla \boldsymbol{u} + \nabla \boldsymbol{u}^T) &\quad \text{in } \Omega, \\
\nabla \cdot \boldsymbol{\lambda} = 0 &\quad \text{in } \Omega, \\
\boldsymbol{\lambda} = \boldsymbol{0} &\quad \text{on } \Gamma_u, \\
\boldsymbol{\lambda} = \boldsymbol{0} &\quad \text{on } \Gamma_d, \\
-\mu \boldsymbol{n} + \nu(\nabla \boldsymbol{\lambda} + \nabla \boldsymbol{\lambda}^T)\boldsymbol{n} + (\boldsymbol{u} \cdot \boldsymbol{n})\boldsymbol{\lambda} = -\nu(\nabla \boldsymbol{u} + \nabla \boldsymbol{u}^T)\boldsymbol{n} &\quad \text{on } \Gamma_N,
\end{aligned} \tag{3.7}$$

[4]The objective functional used in [15] is different from ours. An $\boldsymbol{L}^4$ functional is used for the matching problems and an $\boldsymbol{H}^1_{\Gamma_d}$ is used for the penalization of $\boldsymbol{u}_d$—resulting in a surface Laplacian equation for the decision variables.

and (equation for $\boldsymbol{\tau}$)

$$\nu(\nabla\boldsymbol{\lambda} + \nabla\boldsymbol{\lambda}^T)\boldsymbol{n} + \nu(\nabla\boldsymbol{u} + \nabla\boldsymbol{u}^T)\boldsymbol{n} - \boldsymbol{\tau} = \boldsymbol{0} \quad \text{on } \Gamma_d. \tag{3.8}$$

We may also determine that the strong form of the decision equation is given by

$$\boldsymbol{\tau} = \rho\boldsymbol{d} \quad \text{on } \Gamma_d. \tag{3.9}$$

In [15] estimates are given for the convergence rates of the finite element approximations to the exact solutions for the optimal control of steady viscous flow. For the case of boundary velocity control, the basic result is that if the exact solutions are smooth enough, then provided the Taylor–Hood element is used (for both adjoints and states), the solution error satisfies the following estimates:

$$\begin{aligned} \|\boldsymbol{u} - \boldsymbol{u}_h\|_0 &\leq \mathcal{O}(h^3), \\ \|p - p_h\|_0 &\leq \mathcal{O}(h^2), \\ \|\boldsymbol{\lambda} - \boldsymbol{\lambda}_h\|_0 &\leq \mathcal{O}(h^3), \\ \|\mu - \mu_h\|_0 &\leq \mathcal{O}(h^2). \end{aligned} \tag{3.10}$$

Here h is the maximum element size, and $\|\cdot\|_0$ is the $L^2(\Omega)$ norm.

3.2. Discrete and discretized optimality conditions. In our implementation we have not discretized the continuous forms of the optimality conditions. Instead we have discretized the objective function and the Navier–Stokes equations and then used this discretization to form the optimality conditions. In general, discretization and differentiation (to obtain optimality conditions) do not commute. That is, if $\boldsymbol{A}$ is the infinite-dimensional (linearized) forward operator and $\boldsymbol{A}^*$ is its adjoint, then in general

$$(\boldsymbol{A}^*)_h \neq (\boldsymbol{A}_h)^T,$$

where the subscript h indicates discretization. We will show that for Galerkin approximation of the steady incompressible Navier–Stokes optimal control problem, discretization and differentiation do commute.

For the discretized equations we use the following notation:

$$\begin{aligned} a(\boldsymbol{u}_h, \boldsymbol{v}_h) + c(\boldsymbol{u}_h, \boldsymbol{u}_h, \boldsymbol{v}_h) &\dashrightarrow \mathbf{U}(\mathbf{u})\mathbf{u}, \\ a(\boldsymbol{u}_h, \boldsymbol{v}_h) + c(\boldsymbol{p}_h, \boldsymbol{u}_h, \boldsymbol{v}_h) + c(\boldsymbol{u}_h, \boldsymbol{p}_h, \boldsymbol{v}_h) &\dashrightarrow \mathbf{V}(\mathbf{u})\mathbf{p}, \\ a(\boldsymbol{u}_h, \boldsymbol{v}_h) &\dashrightarrow \mathbf{Qu}, \\ b(q_h, \boldsymbol{u}_h) &\dashrightarrow \mathbf{Pu}, \\ (\boldsymbol{t}_h, \boldsymbol{u}_h)_{\Gamma_d} &\dashrightarrow \mathbf{Tu}, \\ (d_h, r_h)_{\Gamma_d} &\dashrightarrow \mathbf{Md}. \end{aligned}$$

The discretized form of the Navier–Stokes equations (3.2) is then given by

$$\begin{aligned} \mathbf{U}(\mathbf{u})\mathbf{u} + \mathbf{P}^T\mathbf{p} + \mathbf{T}^T\boldsymbol{\sigma} &= \mathbf{f}_1, \\ \mathbf{Pu} &= \mathbf{f}_2, \\ \mathbf{Tu} &= \mathbf{Td}. \end{aligned} \tag{3.11}$$

The discrete Lagrangian function is given by

$$\begin{aligned}\frac{1}{2}\mathbf{u}^T\mathbf{Q}\mathbf{u} + \frac{\rho}{2}\mathbf{d}^T\mathbf{M}\mathbf{d} + \boldsymbol{\lambda}^T\{\mathbf{U}(\mathbf{u})\mathbf{u} + \mathbf{P}^T\mathbf{p} + \mathbf{T}^T\boldsymbol{\sigma} - \mathbf{f}_1\}\\ + \boldsymbol{\mu}^T\{\mathbf{P}\mathbf{u} - \mathbf{f}_2\} + \boldsymbol{\tau}^T\{\mathbf{T}\mathbf{u} + \mathbf{T}\mathbf{d}\} = \mathbf{0}.\end{aligned} \tag{3.12}$$

By taking derivatives with respect to the discrete Lagrange multiplier vectors $(\boldsymbol{\lambda}, \boldsymbol{\mu}, \boldsymbol{\tau})$, we recover the state equations (3.11). By taking derivatives with respect to the discrete state variables $(\mathbf{u}, \mathbf{p}, \boldsymbol{\sigma})$, we obtain the discrete adjoint equations

$$\begin{aligned}\mathbf{V}^T(\mathbf{u})\boldsymbol{\lambda} + \mathbf{P}^T\boldsymbol{\mu} + \mathbf{T}^T\boldsymbol{\tau} &= -\mathbf{Q}\mathbf{u},\\ \mathbf{P}\boldsymbol{\lambda} &= \mathbf{0},\\ \mathbf{T}\boldsymbol{\lambda} &= \mathbf{0}.\end{aligned} \tag{3.13}$$

These equations correspond to the discretization of (3.5) provided that $\mathbf{V}^T\boldsymbol{\lambda}$ is the discretization of $a(\boldsymbol{\lambda}, \boldsymbol{u}) + c(\boldsymbol{v}, \boldsymbol{u}, \boldsymbol{\lambda}) + c(\boldsymbol{u}, \boldsymbol{v}, \boldsymbol{\lambda})$. The bilinear form $a(\cdot, \cdot)$ is symmetric so we omit it from our discussion. If ϕ denotes the basis function for $\boldsymbol{u}$, ψ_v for $\boldsymbol{v}$, and ψ_λ for $\boldsymbol{\lambda}$, then the (3×3)-block elements for the linearized state and adjoint are

$$\int_\Omega \mathbf{I}\,(\nabla\phi \cdot \boldsymbol{u})\psi_v + (\nabla\boldsymbol{u})\phi\psi_v \; d\Omega \quad \text{state element matrix,}$$

$$\int_\Omega \mathbf{I}\,(\nabla\psi_v \cdot \boldsymbol{u})\psi_\lambda + (\nabla\boldsymbol{u})^T\psi_\lambda\psi_v \; d\Omega \quad \text{adjoint element matrix.}$$

Therefore, the transpose of the discretized (linearized) state equations coincides with the discretization of the adjoint equations, i.e.,

$$(\boldsymbol{A}^*)_h = (\boldsymbol{A}_h)^T.$$

One needs to be careful to use the weak form given by (3.5). If (3.7) were used without employing the reverse integration by parts on the term $c(\boldsymbol{u}, \boldsymbol{v}, \boldsymbol{\lambda})$, this would result in a discretization which is incompatible with the discrete optimization problem (which is what is presented to the optimization algorithm). It would result in an nonsymmetric KKT matrix and would possibly prevent the optimizer from converging to a KKT point. A Petrov–Galerkin formulation would also be incompatible.

In our formulation we do not solve explicitly for $\boldsymbol{\sigma}$ and $\boldsymbol{\tau}$. We approximate both tractions and velocity traces in $\boldsymbol{H}^1(\Gamma_d)$; in this case the stresses can be eliminated. For a discussion on choice of $H^1(\Gamma_d)$ for the stresses see [12]. The resulting equations are equivalent to the formulations described in this section. We use a standard Galerkin approximation scheme (no upwinding) with Taylor–Hood elements to approximate the velocities, the pressures, and their adjoints.

We conclude this section with a remark on continuation. To solve a Navier–Stokes control problem with large Reynolds number, some kind of continuation scheme is usually needed. We first solve a Stokes-flow optimal control problem ($\mathrm{Re}_0 = 0$) and then we progressively increase the Reynolds number by $\mathrm{Re}_{(+)} = \mathrm{Re} + \Delta\,\mathrm{Re}$. One could set $\mathbf{u}_{(+)} = \mathbf{u} + (\partial_{\mathrm{Re}}\mathbf{u})\Delta\,\mathrm{Re}$, where $\partial_{\mathrm{Re}}\mathbf{u}$ can be easily computed through a linearized forward solve. Since we consider only steady flows, we follow [10] and use a fixed $\Delta\,\mathrm{Re}$, and simply set $\mathbf{u}_{(+)} = \mathbf{u}$; i.e., the initial guess at the new Reynolds number is the solution from the previous optimization step. Additionally, quasi-Newton information is carried forward to the next Reynolds number.

4. Numerical results.

In this section we investigate the accuracy, performance, and scalability of the LNKS method via four numerical examples. Numerical approximation and parallel implementation details are described in section 4.1 of part I of this article. First we examine the finite element approximation convergence rates with a problem that has a closed form solution. Then we revisit the Poiseuille flow problem of part I and use it to study the effectiveness of the limited-memory BFGS method as a preconditioner for the reduced Hessian. In both cases we solve for the boundary conditions that reproduce the exact solution by minimizing a matching velocity functional.

We then consider the more challenging problem of the control of a flow around a cylinder. The objective function to be minimized is the rate of energy dissipation functional. We use this problem to study the LNKS line search algorithm, the effectiveness of the Krylov–Schur preconditioner for highly nonlinear problems, and the heuristics we introduced in section 2. The last test problem is the optimal control of a flow around a wing.

4.1. Finite element approximation error. In this section we use a model problem to verify the convergence rate estimates given in the previous section. The velocity and pressure are given by

$$\boldsymbol{u}^*(x,y,z) = \{1-(x^2+y^2)^2, x, -y\}^T, \qquad p^*(x,y,z) = x^2+y^2-z^2,$$

which satisfy the Navier–Stokes equations. We restrict this solution to a cylindrical domain and choose a part of its boundary as the control domain Γ_d. We define the velocity on the circumferential walls to be the decision variables. On Γ/Γ_d we set $\boldsymbol{u} = \boldsymbol{u}^*$. The objective function is given by

$$\mathcal{J}(\boldsymbol{u}, \boldsymbol{u}_d, p) = \frac{1}{2}\int_\Omega (\boldsymbol{u}^* - \boldsymbol{u})^2 \, d\Omega.$$

Since the boundary conditions for $(\boldsymbol{u}, p)$ on Γ/Γ_d are compatible with $(\boldsymbol{u}^*, p^*)$, the values for the objective function and the Lagrange multipliers are equal to zero at the minimum.

Table 4.1 gives convergence rates for the state variables and the Lagrange multipliers. The results are in good agreement with the theoretical predictions. The convergence rate for the velocities and their adjoints is approximately 2.92 (comparing errors between the first and second rows) and 2.96 (comparing errors between the second and third rows). For the pressures and their adjoints the convergence rate is 1.96 and 1.97, respectively.

Table 4.1

Convergence rate of the finite element approximation for a matching velocity problem. Here **n** *is the number of elements and h is the cube root of the volume of the maximum inscribed sphere inside a tetrahedron of the finite element mesh. Near-optimal convergent rates can be observed for the state and adjoint variables.*

n	h	$\\|\boldsymbol{u}^* - \boldsymbol{u}_h\\|_0$	$\\|p^* - p_h\\|_0$	$\\|\boldsymbol{\lambda}^* - \boldsymbol{\lambda}_h\\|_0$	$\\|\mu^* - \mu_h\\|_0$
124,639	0.80	1.34×10^{-4}	2.01×10^{-5}	3.88×10^{-4}	1.76×10^{-5}
298,305	0.53	4.40×10^{-5}	9.00×10^{-6}	1.19×10^{-4}	7.90×10^{-6}
586,133	0.40	1.70×10^{-5}	5.20×10^{-6}	5.00×10^{-5}	4.50×10^{-6}

4.2. Poiseuille flow. The Poiseuille flow is a stable solution of the Navier–Stokes equations for small Reynolds numbers. We use this example to study the effectiveness of the limited-memory BFGS method as a preconditioner for the reduced Hessian. Since the optimization problem is nonlinear, LNKS takes several iterations and curvature information can be built up. Quasi-Newton theory predicts that $\mathbf{B}_z$ approaches $\mathbf{W}_z$ as the iterates get closer to the solution. Therefore, we expect the effectiveness of the preconditioner to improve as the optimization algorithm progresses. We store 30 vectors for the limited-memory BFGS preconditioner.

For this set of tests we fix the size and granularity of the problem. The target Reynolds number is 500. We start at Reynolds number 100 and use a continuation step $\Delta\,\mathrm{Re} = 200$. Continuation is *not* used to initialize the state and control variables, but only to carry BFGS information forward to the next Reynolds number.

The forward problem preconditioner is based on a block factorization

$$\begin{bmatrix} \mathbf{I} & -\mathbf{V}^{-1}\mathbf{P}^T \\ \mathbf{0} & \mathbf{I} \end{bmatrix} \begin{bmatrix} \mathbf{V}^{-1} & \mathbf{0} \\ \mathbf{0} & \mathbf{S}^{-1} \end{bmatrix} \begin{bmatrix} \mathbf{I} & \mathbf{0} \\ -\mathbf{P}\mathbf{V}^{-1} & \mathbf{I} \end{bmatrix},$$

where $\mathbf{S} := -\mathbf{P}\mathbf{V}^{-1}\mathbf{P}^T$ is the Schur complement for the pressure. Based on this factorization, the preconditioner is defined by replacing the exact solves $\mathbf{V}^{-1}$ with domain decomposition approximations $\tilde{\mathbf{V}}^{-1}$. To "invert" the pressure Schur complement $\mathbf{S}$ we use several iterations of the two-step stationary method described in part I (section 3.2).

In QN-RSQP we use QMR for the linearized Navier–Stokes solves, preconditioned with an overlapping additive Schwarz method with ILU(1) in each subdomain.[5] Results for a problem with 21,000 state and 3,900 design variables on 4 processors and for a sequence of three Reynolds numbers are presented in Table 4.2. The number of KKT iterations in LNKS-I reveals the efficacy of the BFGS preconditioner. This number drops from an average 48 iterations to 38. The effect of BFGS in LNKS-II is hidden since the KKT iterations are dominated by the ill-conditioning of the forward and adjoint operators (in LNKS-I these solves are exact in each iteration). Overall, we can observe that LNKS reduces significantly the execution time relative to QN-RSQP.

The Newton solver performed well, requiring just 3 iterations to converge. In these problems we did not use inexact Newton criteria to terminate the KKT solves early; instead they were fully converged at each iteration. No line search was used in the LNKS variants; we used the l_1-merit function for the QN-RSQP.

It is rather surprising that the quasi-Newton approximation works well as a preconditioner within the Newton method, whereas it stagnates when used alone to drive the QN-RSQP method. One explanation could be that the QN-RSQP method in these tests suffered the Maratos effect. In our subsequent tests we switched to a second-order correction method [21, p. 570].

4.3. Flow around a cylinder. All the problems examined so far were useful in verifying certain aspects of the LNKS method, but they are linear or mildly nonlinear. In order to test LNKS further we consider a highly nonlinear problem: that of flow around a cylinder with a dissipation-type objective function. The cylinder is anchored inside a rectangular duct, much like a wind tunnel. A quadratic velocity profile is used as an inflow Dirichlet condition and we prescribe a traction-free outflow. The decision variables are defined to be the velocities on the downstream portion of the cylinder surface. We have investigated flows in the laminar steady-state regime. For exterior problems the transition Reynolds number is 40 but for the duct problem we expect higher Reynolds numbers due to the dissipation from the duct walls.

Figures 1 and 2 illustrate optimal solutions for different Reynolds numbers. LNKS eliminates the recirculation region and secondary flows downstream of the cylinder. In

[5]For definitions of ILU(0) and ILU(1) see [22].

Table 4.2

*Work efficiency of the proposed preconditioners for a Poiseuille flow matching problem for fixed size and fixed granularity as a function of the Reynolds number. Recall that LNKS does not use any preconditioner for the KKT system, LNKS-*I *uses a KKT preconditioner that involves two linearized exact forward/adjoint solves per iteration, and LINKS-*II *uses a KKT preconditioner that involves just the application of the forward problem preconditioner.* Re *is the Reynolds number;* N/QN *denotes the number of outer iterations. The number of iterations for the KKT system is averaged across the optimization iterations. The problem has* 21,000 *state equations and* 3,900 *control variables; results are for* 4 *processors of the T*3*E*-900. *Wall-clock time is in hours.*

Re	Method	N/QN iter	KKT iter	$\|\mathbf{g}_z\|$	Time
100	QN-RSQP	262	—	1×10^{-4}	5.9
	LNK	3	186,000	9×10^{-6}	7.1
	LNKS-I	3	48	9×10^{-6}	3.2
	LNKS-II	3	4,200	9×10^{-6}	1.3
300	QN-RSQP	278	—	1×10^{-4}	6.4
	LNK	3	198,000	9×10^{-6}	7.6
	LNKS-I	3	40	9×10^{-6}	3.1
	LNKS-II	3	4,300	9×10^{-6}	1.4
500	QN-RSQP	289	—	1×10^{-4}	7.3
	LNK	3	213,000	9×10^{-6}	9.0
	LNKS-I	3	38	9×10^{-6}	3.0
	LNKS-II	3	4,410	9×10^{-6}	1.4

order to avoid the excessive suction that we observed in the Stokes case, we imposed Dirichlet boundary conditions on the outflow of the domain. The incompressibility condition prevents the optimizer from driving the flow inside the cylinder.[6]

Our experiments on the Stokes optimal control problem demonstrated the dependence of the performance of the Krylov–Schur iteration on the forward problem preconditioner. Thus before we discuss results on the LNKS algorithm we cite representative performance for the Navier–Stokes forward solver. We use an inexact Newton's method combined with the preconditioner we presented in part I. A block-Jacobi ILU(0) preconditioner is used for the velocity block as well as for the pressure mass matrix (scaled by 1/Re); the latter is used to precondition the pressure Schur complement block. ILU(1) would have been a better choice, but memory limitations prevented us from doing so.[7]

Table 4.3 gives statistics for three different Reynolds numbers and for three different problem sizes. We report the (aggregate) number or Krylov iterations required to converge the Newton solver, the number of Newton iterations, and the total execution time. For these runs we did not use continuation, but we did use an inexact Newton method. The time for a forward solve has increased almost sixfold in comparison with the linear Stokes solver (part I, Table 4.1). However the time *per* Newton iteration is roughly the same as that taken in the linear Stokes case. For example, in the 128 processor problem and for Reynolds number 30, the average (Krylov) iteration count is 1005, whereas in the linear case it is 882. Similarly, the average time per Newton

[6]When Dirichlet conditions are specified everywhere on Γ, then $\int_\Gamma \boldsymbol{u} \cdot \boldsymbol{n}\, d\Gamma$ should be zero. The constraint should be imposed either explicitly or implicitly by using a proper function space. In our implementation we use a penalty approach by modifying the objective function.

[7]Our matrix storage includes the state Jacobian, the Hessian of the constraints, and the Hessian of the objective—substantially more than required for the forward solver. PSC's T3E-900 (which hosted the majority of our computations) has just 128 MB of memory per processor.

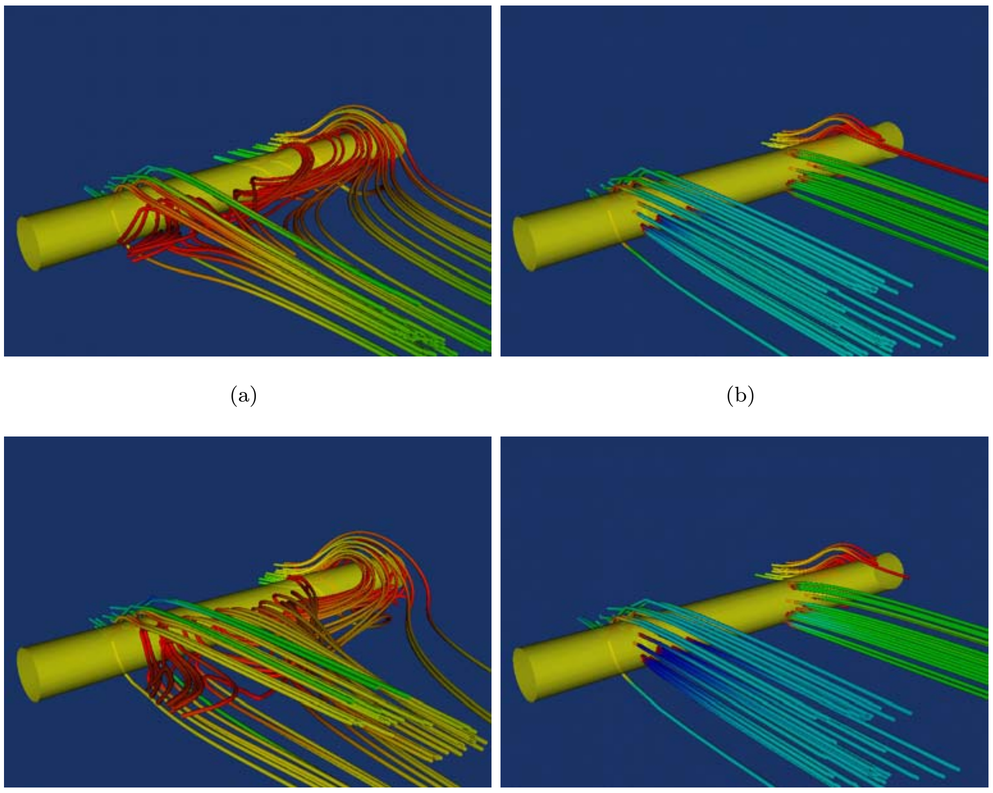

(a) (b)

(c) (d)

FIG. 1. *The top row depicts stream tubes of the flow for Reynolds number* 20 *and the bottom row for Reynolds number* 40. *The left column depicts the uncontrolled flow. The right column depicts the controlled flow. These images illustrate the flow pattern on the downstream side of the cylinder.*

step is 401 seconds. The time for the Stokes solver is little higher, 421 seconds.[8] We conclude that the forward preconditioner performs reasonably well.

Table 4.4 shows results for 32, 64, and 128 processors of a T3E-900 for increasing problem sizes. Results for two different preconditioning variants of LNKS are presented: the exact (LNKS-I) and inexact (LNKS-II) version of the Schur preconditioner. The globalized LNKS algorithm is compared with QN-RSQP. In LNKS-II-TR we activate the inexact Newton method. In this example we have used continuation to warm start the $\mathrm{Re} = 60$ problem. The reduced Hessian preconditioner is a combination of the BFGS and two-step preconditioners (as we described in part I, section 3.2). In the line search we use the augmented Lagrangian merit function.

Based on the overall wall-clock time reported in the rightmost column of Table 4.4, we observe that for this problem, QN-RSQP was able to converge, but only several days of wall-clock time. LNKS-I, although faster, does not reduce the required time significantly. LNKS-II, which avoids the exact forward/adjoint solves, is much

[8]The reason for this is related to the scaling between the velocity and pressure block of the forward problem. Increasing the Reynolds number improves this scaling and thus improves the eigenvalue distribution. Of course this is true up to certain Reynolds number. For higher values the Jacobian becomes highly nonsymmetric and ill-conditioned.

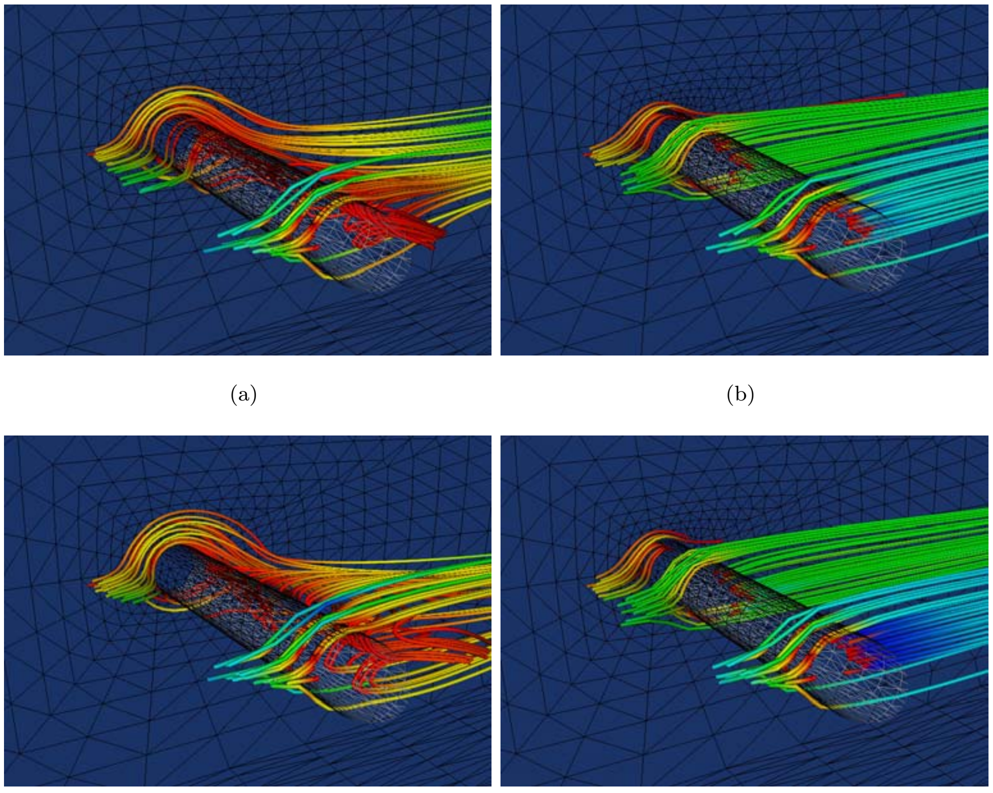

FIG. 2. *The top row depicts stream tubes of the flow for Reynolds number* 20 *and the bottom row for Reynolds number* 40*. The left column depicts the uncontrolled flow. The right column depicts the controlled flow. The decision variables are Dirichlet boundary conditions for the velocities on the downstream half of the cylinder surface. Here we see the flow from the upstream side of the cylinder. In* (c) *we can clearly identify the two standing vortices formed on the lower left corner of the image.*

TABLE 4.3
Forward solver efficiency in relation to problem size and Reynolds number for three-dimensional flow around a cylinder. PEs *is processor number;* n *is the problem size;* Re *is the Reynolds number;* qmr *is the number of aggregate Krylov iterations required to satisfy* $\|\boldsymbol{r}\|/\|\boldsymbol{r}_0\| \leq 1 \times 10^{-7}$*;* nw *is the number of Newton steps to satisfy* $\|\boldsymbol{c}\|/\|\boldsymbol{c}_0\| \leq 1 \times 10^{-6}$*; and* t *is time in seconds. The runs were performed on a T3E-*900*.*

		Re = 20			Re = 30			Re = 60		
PEs	n	qmr	nw	t	qmr	nw	t	qmr	nw	t
32	117.048	2,905	5	612	3,467	7	732	2,850	6	621
64	389,440	4,845	5	1,938	5,423	7	2,101	5,501	7	2,310
128	615,981	6,284	5	2,612	8,036	8	3,214	7,847	7	3,136

better—4 to 5 times faster than QN-RSQP. Even more dramatic is the acceleration achieved by using the inexact version of LNKS, i.e., LNKS-II-TR. The inexactness did not interfere at any point with the merit function and in all cases we observed quadratic convergence. Overall, LNKS-II-TR runs more than 10 times faster than

Table 4.4

The table shows results for 32, 64, *and* 128 *processors of a Cray T3E for a roughly doubling of problem size. Results for the QN-RSQP and LNKS algorithms are presented.* QN-RSQP *is quasi-Newton reduced-space SQP;* LNKS-I *requires two exact linearized forward/adjoint solves per Krylov step combined with the two-step-stationary-BFGS preconditioner for the reduced Hessian; in* LNKS-II *the exact solves have been replaced by approximate solves;* LNKS-II-TR *uses an exact Newton method that avoids fully converging the KKT system for iterates that are far from a solution.* Time *is wall-clock time in hours on a T3E-*900. *Continuation was used only for* Re = 60.

Re = 30

States Controls	Method	N or QN iter	Average KKT iter	Time (hours)
117,048	QN-RSQP	161	—	32.1
2,925	LNKS-I	5	18	22,8
(32 procs)	LNKS-II	6	1,367	5,7
	LNKS-II-TR	11	163	1.4
389,440	QN-RSQP	189	—	46.3
6,549	LNKS-I	6	19	27.4
(64 procs)	LNKS-II	6	2,153	15.7
	LNKS-II-TR	13	238	3.8
615,981	QN-RSQP	204	—	53.1
8,901	LNKS-I	7	20	33.8
(128 procs)	LNKS-II	6	3,583	16.8
	LNKS-II-TR	12	379	4.1

Re = 60

States Controls	Method	N or QN iter	Average KKT iter	Time (hours)
117,048	QN-RSQP	168	—	33.4
2,925	LNKS-I	6	20	31,7
(32 procs)	LNKS-II	7	1,391	6,8
	LNKS-II-TR	11	169	1.5
389,440	QN-RSQP	194	—	49.1
6,549	LNKS-I	8	21	44.2
(64 procs)	LNKS-II	7	2,228	18.9
	LNKS-II-TR	15	256	4.8
615,981	QN-RSQP	211	—	57.3
8,901	LNKS-I	8	22	45.8
(128 procs)	LNKS-II	8	3,610	13.5
	LNKS-II-TR	16	383	5.1

QN-RSQP (5.1 hours compared to 57.3 hours). This is consistent with the performance improvements we observed for the Stokes flow control problem.

Despite the high degree of nonlinearity of the external cylinder flow problem, the augmented Lagrangian globalization performed robustly and we did not have problems converging the optimality equations. In this example, the QN-RSQP safeguard was never activated due to detection of a negative curvature direction. Finally, it is worth noting that the optimization solution is found at a cost of 5 *to* 6 *flow simulations*—remarkable considering that there are thousands of control variables.

4.4. Flow around a Boeing 707 wing. For our last test we solved for the optimal flow control around a Boeing 707 wing. In this problem the control variables

TABLE 4.5

In this table we present results for the wing flow problem, which has 710,023 *state and* 4,984 *decision variables. The runs were performed on* 128 *processors on a T*3*E*-900. *Here* Re *is the Reynolds number;* iter *is the aggregate number of Lagrange–Newton iterations—the number in parentheses is the number of iterations in the last continuation step;* time *is the overall time in hours;* qn *is the number of QN-RSQP steps taken as a safeguard for Newton (the number in parentheses reports the number times a negative curvature was detected);* minc *is the number of nonmonotone line search iterations—in parentheses is the number of times this heuristic failed. The globalized LNKS*-II-*TR algorithm is used. The Lagrange–Newton solver was stopped after* 50 *iterations. In the last column* $\mathrm{Re} \times \Delta f$ *gives the reduction of the objective function (with the respect the uncontrolled flow). "no cont" means that continuation was not activated.*

Re	Iter	Time	qn	Minc	$\|\mathbf{g} + \mathbf{A}^T\boldsymbol{\lambda}\|$	$\|\mathbf{c}\|$	$\mathrm{Re} \times \Delta f$
100 no cont	19	4.06	2	4	9×10^{-6}	9×10^{-6}	4.065
cont							
200 no cont	39	7.8	6(1)	2	9×10^{-6}	9×10^{-6}	5.804
cont	20(10)	4.6	0	3	9×10^{-6}	9×10^{-6}	5.805
300 no cont	48	11.8	16(3)	0	9×10^{-6}	9×10^{-6}	6.012
cont	29(11)	6.4	0	2	9×10^{-6}	9×10^{-6}	6.016
400 no cont	50	13.6	40(3)	0	2×10^{-4}	3×10^{-3}	3.023
cont	33(11)	7.36	0	6(1)	9×10^{-6}	9×10^{-6}	8.345
500 no cont	50	16.7	42(5)	0	4×10^{-2}	9×10^{-2}	1.235
cont	39(14)	9.09	1	5(1)	9×10^{-6}	9×10^{-6}	10.234

are the velocities (Dirichlet conditions) on the downstream half of the wing. The Reynolds number (based on the length of the wing root) was varied from 100 to 500, and the angle of attack was fixed at 12.5 degrees. The problem size is characterized by 710,023 state variables and 4,984 control variables.

Table 4.5 summarizes the results from this set of experiments. The main purpose of this analysis is to compare continuation with the other globalization techniques. In addition we employ the double inexactness idea; that is, we solve inexactly in both the continuation loop and the Lagrange–Newton loop. It is apparent that the use of continuation is crucial in this problem. Without it, and for Reynolds numbers larger than 300, LNKS was forced to terminate early (we set the Lagrange–Newton iteration bound to 50). In the last row (Re = 500) and when we did not use continuation, LNKS ends up switching to a QN-RSQP step 42 times out of a total of 50 iterations; a negative curvature direction was detected 5 times. As a result LNKS was terminated without satisfying the convergence criteria. Furthermore, the small reduction in the objective function and the residuals (last three columns) indicate small progress at each optimization step. Note that in these examples we did not activate backtracking in the continuation parameter.

It could be argued that a reason the algorithm stagnated was the early termination of the Krylov–Schur solver due to inexactness. We did not conduct exhaustive experiments to confirm or reject this. However, our experience on numerous problems suggests that it is the ill-conditioning and nonlinearity of these problems that leads to stagnation and not the inexactness. In our tests (systematic or during debugging and development) it was never the case that a run with exact solves converged in reasonable time, and the inexact version did not. On the contrary, inexactness significantly reduced execution times.

On the other hand, when we used continuation (consisting of relatively large steps on the Reynolds number), the algorithm converged successfully after 39 Lagrange–Newton iterations. Reverting to QN-RSQP was required just once. In the minc column of Table 4.5 we monitor the nonmonotone line search criterion. Recall that if the merit function line search on the LNKS step fails, we perform a line search with a different merit—the KKT residual (i.e., the first-order optimality conditions). If the step gets accepted, via backtracking, we use it as an update direction. Eventually, we insist that the (augmented Lagrangian) merit gets reduced. This strategy was successful 20 times and failed only twice.[9]

Finally we conclude with some comments on the physics of this problem. Figures 3 and 4 depict snapshots of the uncontrolled and controlled flow for Reynolds number 500. The wing-tip vortices are eliminated by optimization. But at what cost? Figure 5 shows a snapshot of the (scaled) control variables—the velocity boundary conditions. The image illustrates that optimization has created a perforated wing, which means a significant reduction in lift (the plane will never leave the ground!). Changing the problem to include a penalty on reduction in lift would remedy the difficulty; this example demonstrates the importance of including all relevant desired goals in the objective, lest optimization defeat them.

5. Conclusions.

In this second part of our two-part article on the LNKS method for PDE-constrained optimization, we have presented the algorithmic components of the (outer) Lagrange–Newton solver, including such globalization strategies as line search, quasi-Newton safeguarding, and parameter continuation, and inexactness in the inner linear solver and its interaction with the line search. We studied the application of the LNKS method to a set of challenging viscous flow optimal boundary control problems that included such compounding factors as three-dimensional unstructured meshes, multicomponent coupling, large problem size, nonlinearity, and ill-conditioning. Our experiments demonstrate the efficacy and scalability of the LNKS method. The Krylov–Schur preconditioner maintained its effectiveness, the Lagrange–Newton solver exhibited mesh-independent convergence, and inexact Newton steps dramatically accelerated the method. A combination of line searching, quasi-Newton safeguarding, and continuation ensured global convergence.

The results reveal at least an order of magnitude improvement in solution time over popular quasi-Newton RSQP methods, rendering tractable some three-dimensional problems with close to a million state variables and several thousand control variables on parallel computers. Indeed, the optimum is often found in a *small* multiple of the cost of a single simulation.

The LNKS method is more suitable for steady PDE constraints. Although the method is in principle applicable to time-dependent problems, it is not recommended for three-dimensional unsteady problems: because LNKS sees the entire space-time domain, it requires large memory for the state and adjoint variables. Moreover, the opportunities for economizing by hiding the nonlinear and linear forward iterations behind the optimization iterations are limited, since the nonlinear systems at each time step are usually mildly nonlinear and well-conditioned (for time-accurate integration). We are investigating various ways to address this issue. Another important extension of LNKS is the treatment of inequality constraints via interior point methods.

Acknowledgments. We thank the PETSc development group at Argonne National Lab for making this work possible. We also thank Jonathan Shewchuk for providing the meshing and partitioning routines Pyramid and Slice, and David Marcum for providing the meshing module AFLR. Finally, we thank David Keyes, David

[9]In general, using the residual of the KKT conditions to test a step can compromise robustness since the optimizer may become trapped in a saddle point or a local maximum.

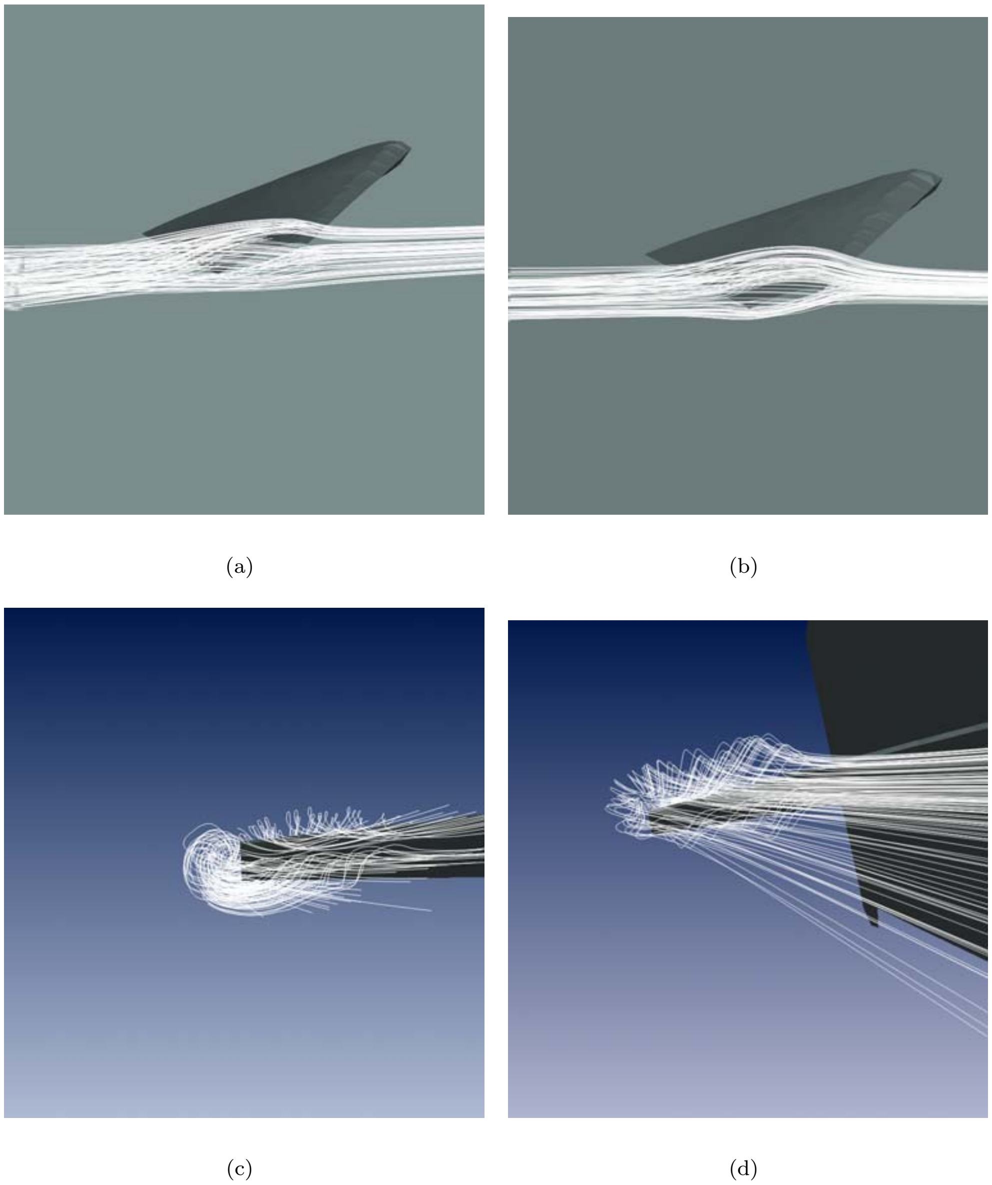

Fig. 3. *The left column depicts streamlines of the uncontrolled flow, while the right depicts streamlines of the controlled flow. Top row gives a side snapshot of the flow; bottom row gives a front view. The Reynolds number (based on the length of the root of the wing) is* 500.

Young of Boeing, and the other members of the TAOS project—Roscoe Bartlett, Larry Biegler, and Andreas Wächter—for their useful comments.

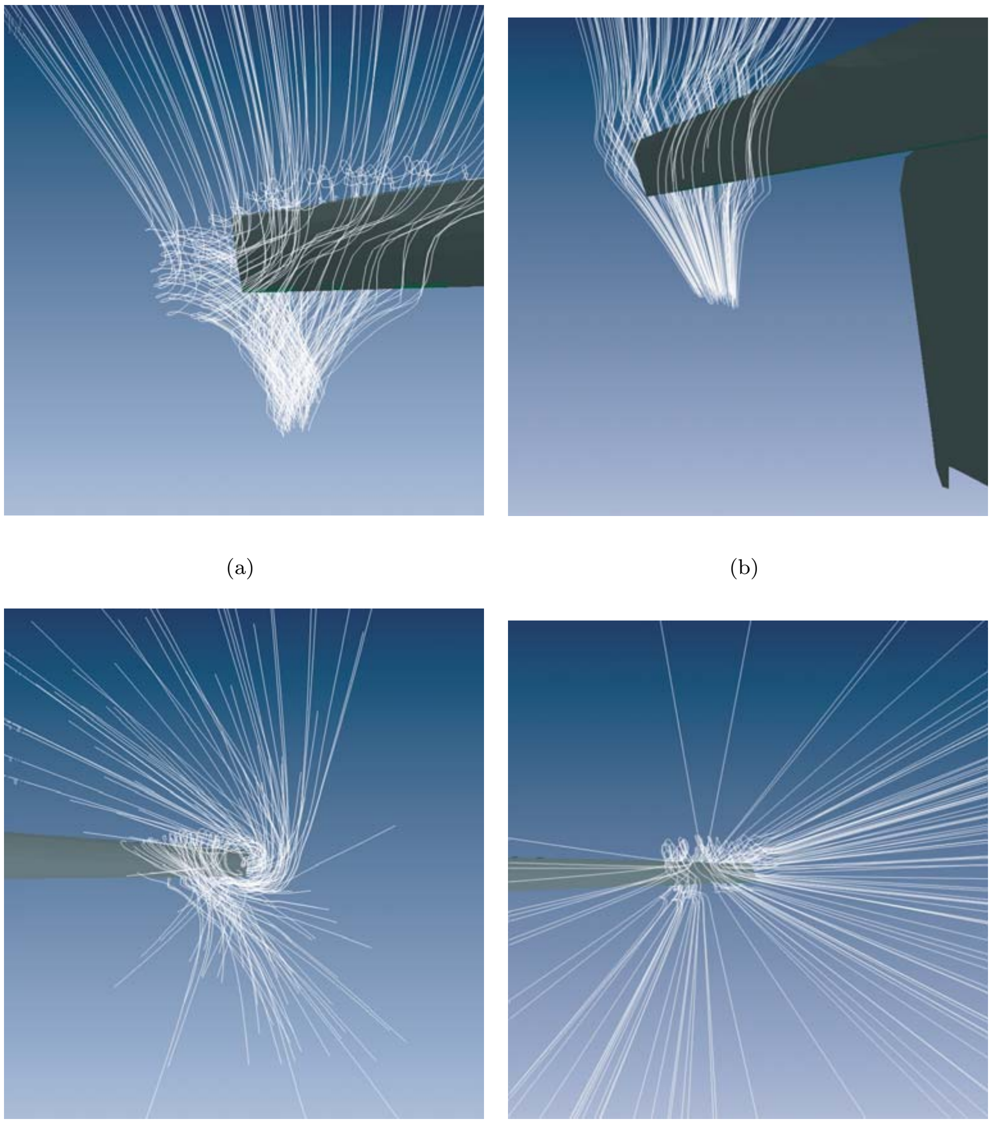

(a) (b)

(c) (d)

FIG. 4. *The left column depicts streamlines of the uncontrolled flow. The right column depicts streamlines of the controlled flow. Top row gives a snapshot of the flow from below; bottom row gives a rear view. Reynolds number is* 500*. We can clearly identify the wing tip vortices in the left images. The images in the right column depict the flow with the wing boundary conditions modified by optimization; the vorticity is eliminated (but so is the lift, since it does not enter into the objective function).*

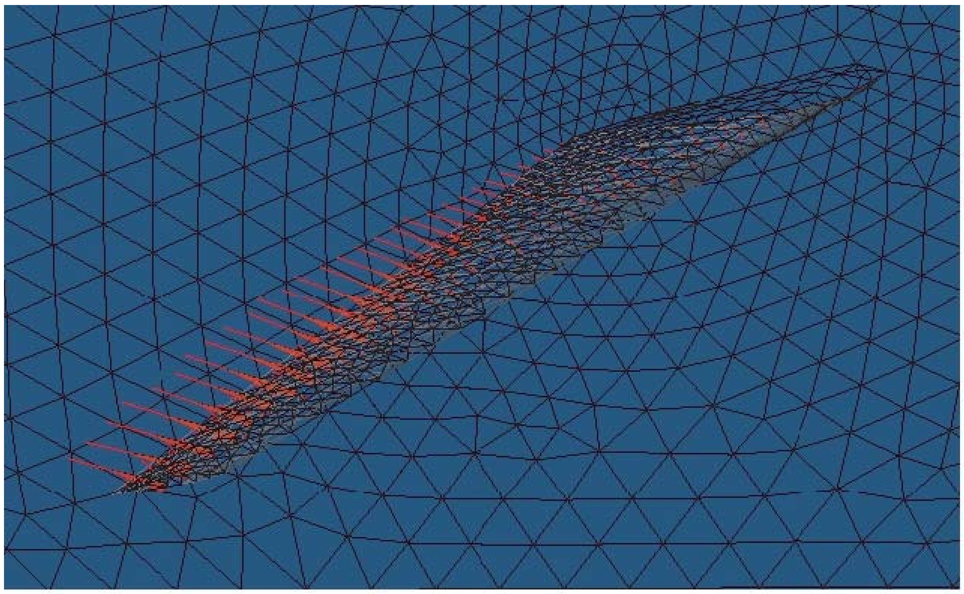

FIG. 5. *Snapshot of the (Dirichlet control) velocity field on the wing.*

REFERENCES

[1] E. L. ALLGOWER AND K. GEORG, *Introduction to Numerical Continuation Methods*, SIAM, Philadelphia, 2003.

[2] I. BABUŠKA, *The finite element method with Lagrangian multipliers*, Numer. Math., 20 (1973), pp. 179–192.

[3] G. BIROS AND O. GHATTAS, *Parallel Lagrange–Newton–Krylov–Schur methods for PDE-constrained optimization. Part* I: *The Krylov–Schur solver*, SIAM J. Sci. Comput., 27 (2005), pp. 687–713.

[4] P. T. BOGGS AND J. W. TOLLE, *A strategy for global convergence in a sequential quadratic programming algorithm*, SIAM J. Numer. Anal., 26 (1989), pp. 600–623.

[5] J. E. DENNIS, JR., M. EL-ALEM, AND M. C. MACIEL, *A global convergence theory for general trust-region-based algorithms for equality constrained optimization*, SIAM J. Optim., 7 (1997), pp. 177–207.

[6] S. C. EISENSTAT AND H. F. WALKER, *Globally convergent inexact Newton methods*, SIAM J. Optim., 4 (1994), pp. 393–422.

[7] S. C. EISENSTAT AND H. F. WALKER, *Choosing the forcing terms in an inexact Newton method*, SIAM J. Sci. Comput., 17 (1996), pp. 16–32.

[8] R. FLETCHER, *Practical Methods of Optimization*, 2nd ed., John Wiley and Sons, Chichester, UK, 1987.

[9] P. E. GILL, W. MURRAY, AND M. H. WRIGHT, *Practical Optimization*, Academic Press, London, New York, 1981.

[10] M. D. GUNZBURGER, *Finite Element Methods for Viscous Incompressible Flows*, Academic Press, Boston, 1989.

[11] M. D. GUNZBURGER, ED., *Flow Control*, IMA Vol. Math. Appl. 68, Springer-Verlag, New York, 1995.

[12] M. D. GUNZBURGER AND S. L. HOU, *Treating inhomogeneous essential boundary conditions in finite element methods and the calculation of boundary stresses*, SIAM J. Numer. Anal., 29 (1992), pp. 390–424.

[13] M. D. GUNZBURGER AND R. A. NICOLAIDES, EDS., *Incompressible Computational Fluid Dynamics*, Cambridge University Press, Cambridge, UK, 1993.

[14] M. HEINKENSCHLOSS AND L. N. VICENTE, *Analysis of Inexact Trust-Region SQP Algorithms*, Technical report TR99-18, Department of Computational and Applied Mathematics, Rice University, Houston, TX, 1999.

[15] L. S. Hou, *Analysis and Finite Element Approximation of Some Optimal Control Problems Associated with the Navier-Stokes Equations*, Ph.D. thesis, Carnegie Mellon University, Pittsburgh, PA, 1989.
[16] L. S. Hou and S. S. Ravindran, *Numerical approximation of optimal flow control problems by a penalty method: Error estimates and numerical results*, SIAM J. Sci. Comput., 20 (1999), pp. 1753–1777.
[17] C. T. Kelley and E. W. Sachs, *Truncated Newton methods for optimization with inaccurate functions and gradients*, J. Optim. Theory Appl., 116 (2003), pp. 83–98.
[18] C. T. Kelley and D. E. Keyes, *Convergence analysis of pseudo-transient continuation*, SIAM J. Numer. Anal., 35 (1998), pp. 508–523.
[19] F. Leibfritz and E. W. Sachs, *Inexact SQP interior point methods and large scale optimal control problems*, SIAM J. Control Optim., 38 (1999), pp. 272–293.
[20] S. G. Nash and A. Sofer, *Linear and Nonlinear Programming*, McGraw-Hill, New York, 1996.
[21] J. Nocedal and S. J. Wright, *Numerical Optimization*, Springer-Verlag, New York, 1999.
[22] Y. Saad, *Iterative Methods for Sparse Linear Systems*, PWS, Boston, 1996.
[23] K. Schittkowski, *The nonlinear programming method of Wilson, Han, and Powell with an augmented Lagrangian type line search function*, Numer. Math., 38 (1981), pp. 83–114.
[24] T. Steihaug, *The conjugate gradient method and trust regions in large scale optimization*, SIAM J. Numer. Anal., 20 (1983), pp. 626–637.
[25] H. Yamashita, *A globally convergent constrained quasi-Newton method with an augmented Lagrangian type penalty function*, Math. Program., 23 (1982), pp. 75–86.